

AUTOMATIC PRESSURE CONTROL SYSTEM

Gabriela KOREISOVÁ, Josef KOREIS

Department of Means of Transport and Diagnostics

Introduction

The article describes static and dynamic characteristics of the pressure control system of a regulatory hydraulic generator into an open hydraulic circuit. The pressure control system of a hydraulic generator into an open hydraulic circuit, (HGR-O) is schematically outlined on **Fig. 1**.

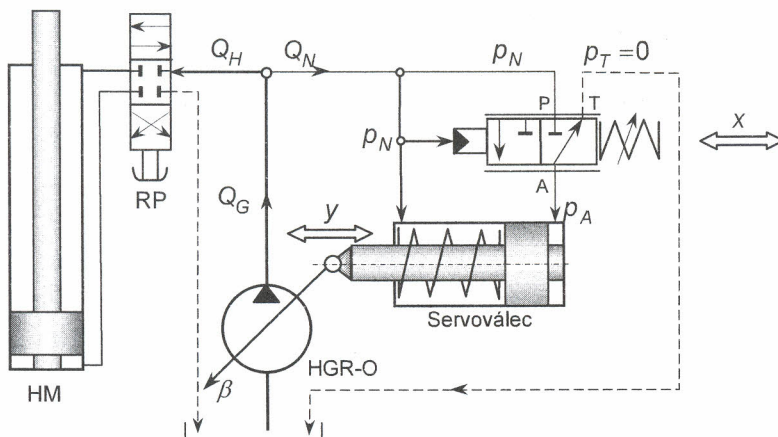


Fig. 1 The pressure control system HGR-O

The basic features of the system are a regulatory hydraulic generator into an open hydraulic circuit (HGR-O), a pressure control unit with a slide valve stroke $x(t)$ and servo-cylinder with a piston-rod stroke $y(t)$. Hydraulic generator supplies output flow Q_G . A part of the flow Q_H runs to the hydraulic motor that constitutes hydraulic generator load while the other part Q_N flows through the control unit and servo-cylinder. In the entire bifurcated output branch there rules the system pressure p_N composed of loading resistors. At the same time, p_N is a feeding pressure of the control unit (brought to the "P" input) and controlled pressure of the system set by the bias of the control unit spring. The required preset value of the controlled pressure is marked with an asterisk in the exponent. If $p_N < p_N^*$, the control unit is out of operation. At the hydraulic generator, the maximal output flow at the maximal geometric volume $\beta = 1$. In the instant when pressure p_N reaches the preset required value the control unit is put into operation. At the control unit "A" output arises non-zero controlling pressure p_A that starts shifting the piston-rod of the servo-cylinder towards the maximal position. The course of the output controlling pressure of the control unit is dependent on geometry of controlling edges of the slide valve and slide valve stroke $x(t)$. ($p_A(t) = f(x(t))$).

1. Arrangement and Parameters of the Pressure Control Unit.

The arrangement of the pressure control unit is outlined on *Fig. 2*. The slide valve features only two spigots. The controlling one and conducting one.

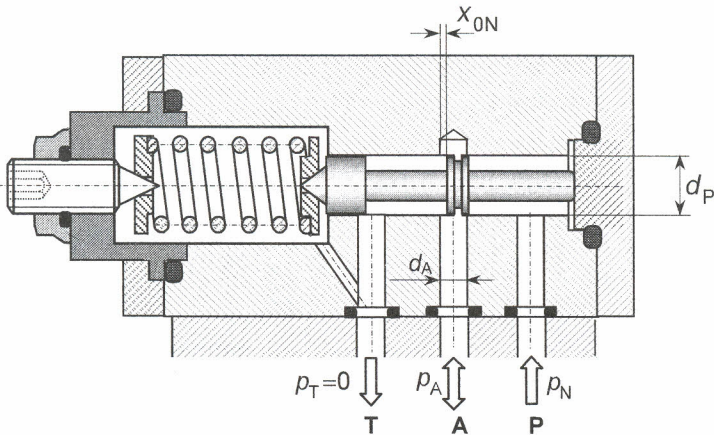


Fig. 2 The arrangement of the pressure control unit

The input controlling edge is closed with zero cover. (In a real-life version, the input controlling edge may be closed against high pressure with non-zero positive cover). The output controlling edge is opened with basic negative cover x_{ON} . The feeding pressure p_N

affects the entire front area of the slide valve of diameter d_p . Hydraulic force $S_p \cdot p_N(t)$ is balanced with the spring force $k \cdot (x_0 + x(t))$. The dependence of the output controlling pressure p_A on the slide valve stroke $x(t)$ is an inner static characteristic of the control unit. The time flow of the slide valve stroke of the control unit $x(t)$ is a basic characteristic of the control unit.

Basic Parameters of the Control Unit:

Nominal diameter of the slide valve	$d_p = 8 \text{ mm}$	area	$S_p = 16 \cdot \pi = 50,254 \text{ mm}^2$
Calculating clearance	$2h = d_{p1} - d_{p2} = 0,0032 \text{ mm}$		
Total length of conducting spigots	$L = 12 \text{ mm}$		
Basic negative cover	$x_{0N} = 0,42 \text{ mm}$	$(x_{0N} = x_{\max})$	
Diameter of controlling hole in body	$d_A = 5 \text{ mm}$		
Calculating weight of the slide valve	$m = 0,01012 \text{ kg}$		
Feeding pressure	$p_N^* = 25 \text{ MPa}$		
Drawback spring rigidity	$k = 273,3 \text{ N} \cdot \text{mm}^{-1}$		
Working oil viscosity	$\mu = 1,45 \cdot 10^{-2} \text{ N} \cdot \text{s} \cdot \text{m}^{-2}$		
Oil specific weight	$\rho = 900 \text{ kg} \cdot \text{m}^{-3}$		

Calculated Dynamic Parameters.

Natural frequency quadrat	$\omega_0^2 = \frac{k}{m} = 27005929 \text{ s}^{-2}$
	$(\omega_0 = 5196,723 \text{ s}^{-1})$
Viscous damping coefficient	$b = \pi \cdot \mu \cdot L \cdot \frac{d_p}{h} = 2,733 \text{ N} \cdot \text{s} \cdot \text{m}^{-1}$

2. Inner Static Characteristic of the Control Unit

Theoretic inner static characteristics may be achieved by calculation, with a constant input feeding pressure. Actual inner static characteristics are determined by measurement. Controlling edges of the slide valve constitute the local hydraulic resistances. Loss in pressure at the controlling edges is proportional to the flow quadrat:

$$\Delta p = \xi \cdot \frac{1}{2} \cdot \rho \cdot v^2 = \frac{\xi \cdot \rho}{2 \cdot S^2} \cdot Q^2 = R \cdot Q^2 \tag{1}$$

Hydraulic resistance:
$$R = \frac{\xi \cdot \rho}{2 \cdot S^2} = \frac{A}{S^2} \tag{2}$$

With the controlling edges of the slide valve, the flow area is a variable dependent on the slide valve stroke x and controlling edges geometry applied. Figure **Fig. 2** outlines the front controlling edges on the controlling spigot of the slide valve and the controlling hole in the the control unit body (Geometry "B"). The flow area is formed by intersection of two cylinder areas. The size of the flow area is calculated as an area of parabolic segment. One concurrent controlling hole constitutes two flow areas on one controlling.

With zero cover of the input controlling edge (**Fig. 2**), it applies for the flow areas:

$$S_1(x) = \frac{8}{3} \sqrt{d_A \cdot x^3}, \quad S_2(x) = \frac{8}{3} \sqrt{d_A \cdot (x_{0N} - x)^3} \quad (3)$$

Connection of resistances of the two-edge controlling slide valve is outlined on **Fig. 3**.

Fig. 3 Controlling Resistances Connection

Static characteristic is dependence of two quantities in several succeeding steady states. In the steady state, there is balance of static forces on the servo-cylinder while the piston-rod is halted. The rate of flow $Q_A(t) = S_V \cdot \dot{y}(t)$ is zero. Then $Q_T = Q_N$ and the entire input flow flows through open controlling edges. On **Fig. 3** flows the flow Q_N through the both controlling holes of the control unit.

it applies for the pressure losses on the controlling resistances on **Fig. 3**:

$$p_N - p_A = R_1 \cdot Q_N^2 = \frac{A}{S_1^2} \cdot Q_N^2, \quad p_A - p_T = R_2 \cdot Q_N^2 = \frac{A}{S_2^2} \cdot Q_N^2 \quad (4)$$

$$p_N - p_T = (R_1 + R_2) \cdot Q_N^2 = \left(\frac{1}{S_1^2} + \frac{1}{S_2^2} \right) \cdot A \cdot Q_N^2 = \frac{S_1^2 + S_2^2}{S_1^2 \cdot S_2^2} \cdot A \cdot Q_N^2 \quad (5)$$

If $p_T = 0$

$$\frac{p_A}{p_N} = \frac{R_2}{R_1 + R_2} = \frac{S_1^2}{S_1^2 + S_2^2} \quad (6)$$

The flow rate through open negative cover of the controlling edges:

$$Q_N = S_2 \cdot \sqrt{\frac{p_A}{A}} = S_1 \cdot \sqrt{\frac{p_N - p_A}{A}} = \frac{S_1 \cdot S_2}{\sqrt{A \cdot (S_1^2 + S_2^2)}} \cdot \sqrt{p_N} \quad (7)$$

Definition of dimensionless quantities:

$$\bar{x} = \frac{x}{x_{\max}} = \frac{x}{x_{0N}}, \quad \bar{p}_A = \frac{p_A}{p_{A\max}} = \frac{p_A}{p_N}, \quad \bar{Q}_N = \frac{Q_N}{Q_{N\max}}$$

If substituted for flow areas according to (3) it applies:

$$\bar{p}_A = \frac{\bar{x}^3}{\bar{x}^3 + (1-\bar{x})^3} \quad (8)$$

Linearly growing slide valve $\bar{x}(t) \in \langle 0; 1 \rangle$ and constant feeding pressure $\bar{p}_N^* = 1$ is substituted in the equation (8) (Theoretic characteristics).

Analogically, the dimensionless flow through open negative cover finds its dependence:

$$\bar{Q}_N = 4 \cdot \sqrt{(1-\bar{x})^3 \cdot \bar{p}_A} \quad (9)$$

Simulation model constructed according to the latter two equations is depicted on **Fig. 4**.

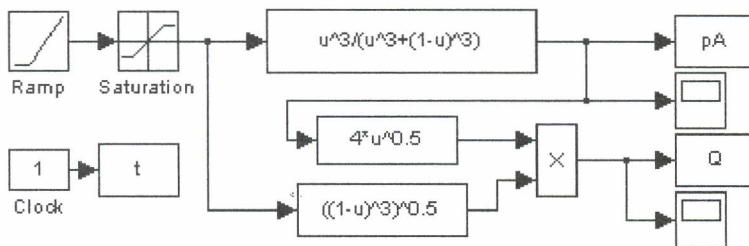


Fig. 4 Simulation model of the dimensionless inner static characteristics of the control unit

The calculation results in dimensionless inner static characteristics of the control unit we can see at **Fig. 5**.

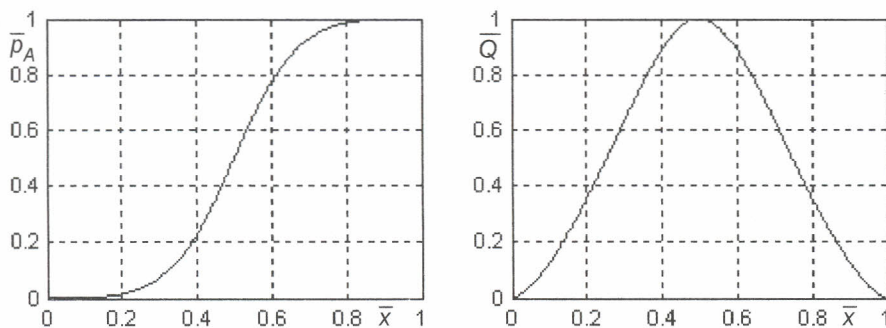


Fig. 5 Dimensionless inner static characteristics of the control unit

On the left there is the pressure and on the right there is the flow dimensionless inner static characteristic of the control unit. With maximal pressure of 25 MPa, maximal losing flow is about 2.5 dm³/min. For controlling is used the middle distance of the pressure characteristic with steepness of $\Delta \bar{p} / \Delta \bar{x} = 3$.

3. Analysis of dynamic characteristics of the control unit

Required value of the controlling pressure is set through drawback spring bias of the control unit according to the static forces balance equation in the initial (zero) position:

$$k \cdot x_0 = S_P \cdot p_N^* \quad (10)$$

Maximal stroke is determined by the size of the basic negative cover $x_{0N} = 0.42 \text{ mm}$. To achieve the maximal stroke, it is necessary to increase the required value of the controlled pressure by static variance Δp_S .

Static forces shall be balanced on the slide valve in the maximal position:

$$(p_N^* + \Delta p_S) \cdot S_P = k \cdot (x_0 + x_{0N}) \quad (11)$$

With the maximal stroke, the controlling pressure has maximal value

$$p_{Amax} = p_N^* + \Delta p_S$$

The time flow of the slide valve stroke is determined through the balance of all static and dynamic forces affecting on the slide valve:

$$(p_N^* + \Delta p_N(t)) \cdot S_P = m \cdot \ddot{x}(t) + b \cdot \dot{x}(t) + k \cdot (x_0 + x(t)) \quad (12)$$

After the initial static forces are eliminated according to (10) the balance of the dynamic forces will result:

$$\Delta p_N(t) \cdot S_P = m \cdot \ddot{x}(t) + b \cdot \dot{x}(t) + k \cdot x(t) \quad (13)$$

It follows from the equations (10) and (11):

$$\Delta p_S = \frac{k}{S_P} \cdot x_{0N} = 2,275 \text{ MPa}, = 0,091 \cdot p_N^* \quad (14)$$

In the kinetic equation (12), the input change of pressure must be of value $\Delta p_N = \Delta p_S$ according to the result (14) so that the slide valve of the control unit moves from the zero position to the maximum position.

For assembling the simulation model, the equation (13) shall be transformed into an operator shape:

$$\Delta p_N(s) \cdot S_P = (m \cdot s^2 + b \cdot s + k) \cdot x(s) = k \cdot (T_2^2 \cdot s^2 + T_1 \cdot s + 1) \cdot x(s) \quad (15)$$

Definition of dimensionless quantities:

$$\bar{x} = \frac{x}{x_{max}} = \frac{x}{x_{0N}}, \bar{p} = \frac{p}{p_{Tmax}}, \Delta \bar{p}_N = \frac{\Delta p_N}{p_N^*} \quad (16)$$

Equation (15) in a dimensionless shape:

$$\Delta \bar{p}_N(s) = \frac{k \cdot x_{0N}}{S_P \cdot p_N^*} (T_2^2 \cdot s^2 + T_1 \cdot s + 1) \cdot \bar{x}(s) \quad (17)$$

Image transmission of the control unit:

$$G_X(s) = \frac{\bar{x}(s)}{\Delta \bar{p}_N(s)} = \frac{\bar{r}_{0X}}{T_2^2 s^2 + T_1 s + 1} = \frac{\bar{r}_{0X}}{T_2^2 s^2 + 2\delta T_2 s + 1} = \frac{\bar{r}_{0X} \cdot \omega_0^2}{s^2 + 2\delta \omega_0 s + \omega_0^2} \quad (18)$$

where:

$$\bar{r}_{0X} = \frac{S_{SP} \cdot p_N^*}{k \cdot x_{0N}} = \frac{1}{\Delta p_{NS}} = 10,94 \dots \dots \dots \text{dimensionless proportional amplification of the control unit,}$$

$$T_2^2 = \frac{m}{k} = \frac{1}{\omega_0^2} = 3,7 \cdot 10^{-8} \text{ (s}^2\text{)} \dots \dots \dots \text{time constant of the second order,}$$

$$T_1 = \frac{b}{k} = \frac{2\delta}{\omega_0} = 10^{-5} \text{ (s)} \dots \dots \dots \text{time constant of the first order.}$$

The relation for the viscous damping coefficient was derived for incompressible Newton liquid with the prerequisite of linear distribution of speeds through clearance and zero pressure loss on the conducting spigot [2].

Numeric values of the basic parameters of the control unit were chosen. Calculated values of the dynamic parameters are just orientational, used for model calculations. After the back control feed is closed and simulation model of the entire pressure control system is assembled, some parameters will be fine-tuned. The stated dependencies of the dynamic parameters on the basic parameters of the control unit facilitate tuning of real control systems at the testing room.

Behind the control unit output $x(t)$ it is now possible to connect a non-linear function $p_A = f(x)$ according to Equation (8). A corresponding simulation model is on **Fig. 6**.

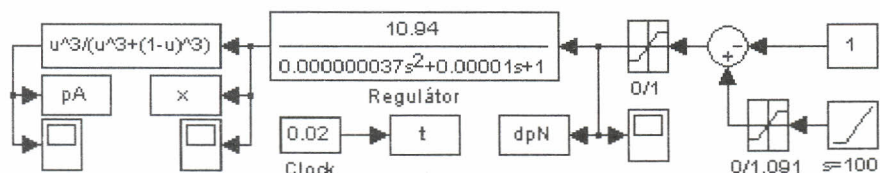


Fig. 6 Simulation model of dynamic properties of the control unit

The result of the simulation is on **Fig. 7**. The time shift is caused by creation of regulatory deviation. Constant -1 is a step change. A ramp of steepness $s=100 \text{ s}^{-1}$ reaches the value +1 in time $t_1 = 0.01 \text{ s}$ when the transitional process begins. In the ramp function it is possible to set the initial value $i = +1$. the entire control unit may be modelled by substitutive P- transfer of the first order, (**Fig. 8**)

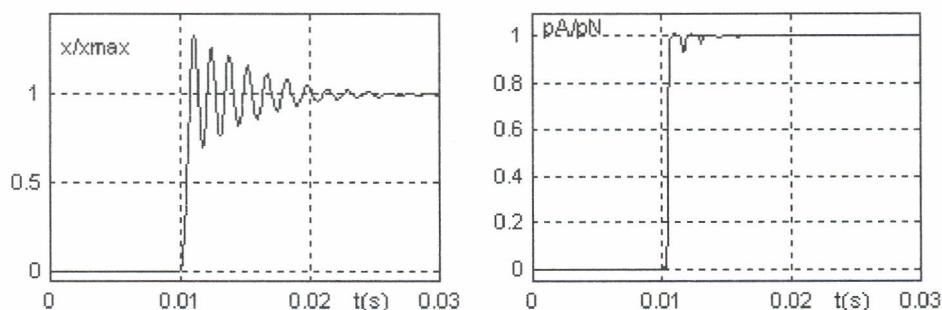


Fig. 7 The time flow of the slide valve stroke and the course of controlling pressure

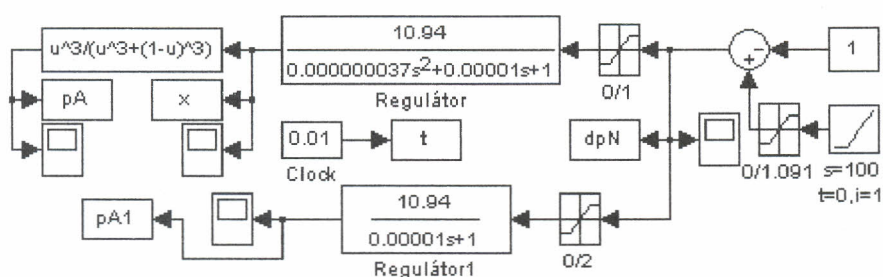


Fig. 8 Substitutive image transmission of the control unit.

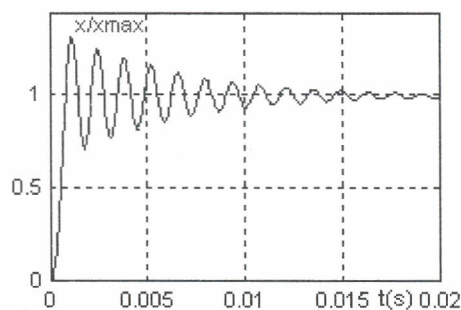


Fig. 9 Slide valve stroke

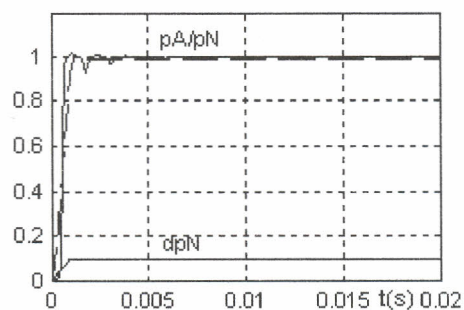


Fig. 10 Substitutive course of the controlling pressure

The course of the slide valve stroke is oscillated. The course of the controlling pressure is not that oscillated. The slide valve may overshoot behind the maximal active position. After the maximal stroke is exceeded, the output controlling edge is closed now

and the controlling pressure p_A cannot be of higher value than the feeding pressure p_N . The calculated superelevation may be cut off by inserting a limiting block in the simulation model on **Fig. 6**. More suitable is application of substitutive course of the controlling pressure through P-shift of the first order, (dashed on **Fig. 10**), according to the model on **Fig. 8**.

4. Arrangement and Parameters of the Servo-cylinder.

For controlling the geometric volume HGR-O, there is a standard servo-cylinder schematically outlined on **Fig. 1** and **Fig. 3** with drawback spring. Realization is depicted on **Fig. 11**.

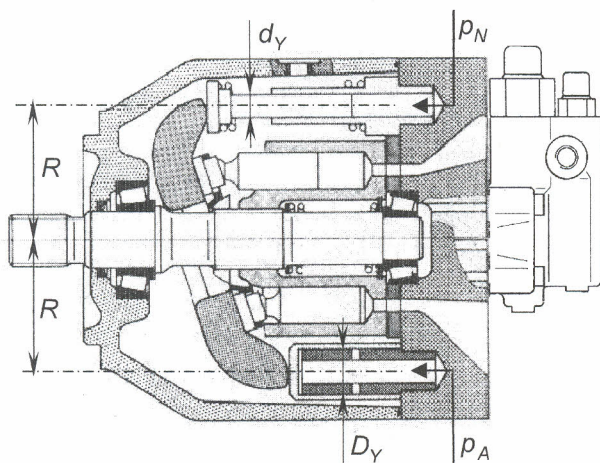


Fig. 11 Arrangement of the controlling servo-cylinder

In the upper part, the drawback spring is placed on an independent piston-rod of diameter d_Y . System pressure p_N affects the area of the piston-rod S_{Y2} .

The controlling piston is hollow, placed on the fixed conduction of diameter D_Y , with active area S_{Y1} and the width of the wall $t=4\text{ mm}$. This is rather different arrangement than on the schematic Figure 1 where the system pressure p_N affects the differential area $S_{Y1} - S_{Y2}$.

Basic Parameters of the Servo-cylinder:

Internal diameter of the piston $D_Y = 34_{-\Delta}^{+0}\text{ mm}$, area $S_{Y1} = 289 \cdot \pi = 907,29\text{ mm}^2$

Diameter of the piston-rod $d_Y = 24_{-0}^{+\Delta}\text{ mm}$, area $S_{Y2} = 144 \cdot \pi = 452,38\text{ mm}^2$

Spring stiffness constant	$k_Y = 133 \text{ N.mm}^{-1}$
Radius of the arm	$R = (2,9 \div 3,1) \cdot D_Y = 96 \text{ mm}$
Maximal angle of the swing board	$\alpha = (19 \div 20)^\circ$
Maximal stroke	$y_{\max} = R \cdot \text{tg } \alpha = 34 \text{ mm}$ (Výpočtová hodnota)
Length of the piston placement	$L_1 \cong 3 \cdot y_{\max} = 100 \text{ mm}$
Length of the piston-rod placement	$L_2 \cong 3 \cdot y_{\max} = 100 \text{ mm}$
Clearance	$h = 0,001 \text{ mm}$

The indicated numeric values of the basic parameters of the servo-cylinder were chosen for analysing. With the real embodiment HGR-0, the basic parameters are known.

Calculated parameters:

Weight of piston and piston-rod	$m_{YT} = 0,908 \text{ kg}$
Weight of the swing board	$m_D = 6,357 \text{ kg}$, inertia moment $J = 0,0162 \text{ kg.m}^2$

Reduced weight of the board $m_{DR} = \frac{J}{R^2} = 1,76 \text{ kg}$

Resulting translation translational weight in the axis of the servo-cylinder:

$$m_Y = m_{YT} + m_{DR} = 2,668 \text{ kg.}$$

Natural frequency $\omega_{0Y} = \sqrt{\frac{k_Y}{m_Y}} = 223,27 \text{ s}^{-1}$ (quadrat $\omega_{0Y}^2 = 49850 \text{ s}^{-2}$)

Ratio of the active surfaces: $S_{Y2} / S_{Y1} = 144 / 289 = 0,498 \cong 0,5$

Viscous damping coefficient (if $\mu = 1,45 \cdot 10^{-2} \text{ N.s.m}^{-2}$)

piston: $b_{1Y} = \pi \cdot \mu \cdot D_Y \cdot \frac{L_1}{h} = 145,77 \text{ N.s.m}^{-1}$

piston-rod: $b_{2Y} = \pi \cdot \mu \cdot d_Y \cdot \frac{L_2}{h} = 100,21 \text{ N.s.m}^{-1}$

Translational movement damping coefficient without being affected by resistance against swing board rotation: $b_{YT} = b_{1Y} + b_{2Y} = 246 \text{ N.s.m}^{-1}$ being affected by resistance against swing board rotation $b_Y = 492 \text{ N.s.m}^{-1}$.

Dimensionless damping factor is $\delta_Y = \frac{b_Y}{2 \cdot \sqrt{k_Y \cdot m_Y}} = 0,413$.

5. Analysis of Static and Dynamic Properties of the Servo-cylinder

Static characteristic of the servo-cylinder is dependence of the stroke $y(t)$ on the controlling pressure $p_A(t)$, in a row of subsequent steady states. Initial relation is the balance of static forces:

$$p_A(t) \cdot S_{Y1} = k_Y \cdot (y_0 + y(t)) + p_N \cdot S_{Y2} \quad (19)$$

Considering that the hydraulic force $p_N \cdot S_{Y2}$ affects in the same direction as the spring force, the spring may be installed with insignificantly minor bias. If $y_0 = 0$ then:

$$p_A(t) \cdot S_{Y1} - p_N \cdot S_{Y2} = S_{Y1} \cdot (p_A(t) - 0,5 \cdot p_N) = k_Y \cdot y(t) \quad (20)$$

As long as the left side of the Equation (20) is negative, then $y = 0$ and the piston stands in the right stop position. Controlling pressure $p_A(t)$ gradually increases up to the start value $p_{A0} = 0,5 \cdot p_{N0}$ when the servo-cylinder starts to move. To make sure that the controlling pressure $p_A(t)$ is nonzero, the slide valve must be opened by pressure $p_N(t) > p_N^*$. To put it simply, it is save to presume that the real controlled pressure will be dimensionless calculating value $\bar{p}_{N0} = 1 + \Delta\bar{p}_{NS} = 1,091$ That provided, the starting pressure will be of dimensionless value:

$$\bar{p}_{A0} = 0,5 \cdot (1 + \Delta\bar{p}_{NS}) = 0,545 \quad (21)$$

Control of servo-cylinder stroke and geometric volume HGR-O is over on maximal stroke with servo-cylinder piston-rod leaning against a terminative position stop. That shall occur on balance of forces.

$$S_{Y1} \cdot (p_{AM} - 0,5 \cdot (p_N + \Delta p_{NS})) = k_Y \cdot y_{\max} \quad (22)$$

Limit pressure at the end of control will be of value:

$$\bar{p}_{AM} = \frac{k_Y \cdot y_{\max}}{p_N^* \cdot S_{Y1}} + \bar{p}_{A0} = 0,866 \quad (23)$$

It is not necessary to model the limit controlling pressure $\bar{p}_{AM} = 0,866$. More expedient is to model a mechanical stop of the piston-rod at the value y_{\max} .

From Equation (20) it follows for the servo-cylinder stroke:

$$y(t) = \frac{S_{Y1}}{k_Y} \cdot (p_A(t) - 0,5 \cdot p_N(t)) = \frac{S_{Y1}}{k_Y} \cdot (p_A(t) - 0,5 \cdot (p_N^* + \Delta p_N(t))) \quad (24)$$

In a dimensionless shape:

$$\bar{y}(t) = \frac{S_{Y1} \cdot p_N^*}{k_Y \cdot y_{\max}} \cdot (\bar{p}_A(\bar{x}(t)) - 0,5 \cdot (\bar{p}_N^* + \Delta \bar{p}_N(t))) \quad (25)$$

Here is generally $\bar{p} = \frac{p}{p_{\max}}$ and specially $\bar{p}_A = \frac{p_A}{p_{A\max}} = \frac{p_A}{p_N}$, $\bar{p}_N^* = \frac{\bar{p}_N^*}{\bar{p}_{N\max}}$ (26)

All the existing calculations were done for the required value of the controlled pressure $\bar{p}_N^* = 1$. Static characteristics of the servo-cylinder will be calculated for lower required values of the controlled pressure. In the relation (25), dependence (8) shall be substituted for $\bar{p}_A(\bar{x}(t))$, modified also for decreased values of the controlled pressure.

The result of the calculation according to (25) shall be converted through applying the relation $\beta(t) = 1 - \bar{y}(t)$ to controlled pressure dependence on the geometric volume (Fig. 12).

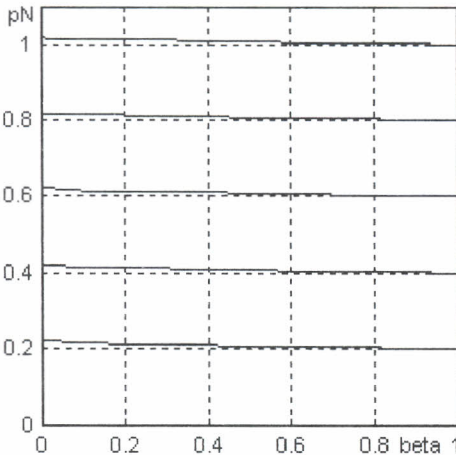


Fig. 12 Static characteristics of the servo-cylinder.

Similar static characteristics are quoted by HGR-O producers in the technical documentation, usually in a dimensionless shape. On Fig. 11, there are static characteristics outlined for several required values of the controlled pressure. With a zero servo-cylinder stroke and maximal geometric HGR volume, each characteristic starts on the required value of the controlled pressure.

With decreasing geometric volume and increasing servo-cylinder stroke, the drawback spring gets pressed while the controlled pressure increases by a static deviation. With zero geometric volume and maximal stroke, the static deviations are maximal. (For better clearness, the static deviations on Fig. 12 were increased).

Dynamic characteristic of the servo-cylinder, (the time flow of the stroke $y(t)$), is determined through the balance of all the forces:

$$(p_A(t) - 0,5 \cdot p_N(t)) \cdot S_{Y1} = k_Y \cdot y(t) + b_Y \cdot \dot{y}(t) + m_Y \cdot \ddot{y}(t) \quad (27)$$

For dimensionless quantities in the operator shape.

$$\bar{p}_A(s) - 0,5 \cdot (1 + \Delta \bar{p}_N(s)) = \Delta p_R(s) = \frac{k_Y \cdot y_{\max}}{S_{Y1} \cdot p_N^*} \cdot \left(1 + \frac{b_Y}{k_Y} \cdot s + \frac{m_Y}{k_Y} \cdot s^2 \right) \cdot \bar{y}(s) \quad (28)$$

Image transmission of the servo-cylinder:

$$G_Y(s) = \frac{y(s)}{\Delta p_R(s)} = \frac{\bar{r}_{0Y}}{T_{2Y}^2 \cdot s^2 + T_{1Y} \cdot s + 1} \quad (29)$$

where:

$$\bar{r}_{0Y} = \frac{S_{Y1} \cdot p_N^*}{k_Y \cdot y_{\max}} = 5 \quad \dots \dots \dots \text{dimensionless proportional amplification of the servo-cylinder,}$$

$$T_{2Y}^2 = \frac{m_Y}{k_Y} = \frac{1}{\omega_{0Y}^2} = 2 \cdot 10^{-5} \text{ (s}^2\text{)} \quad \dots \dots \dots \text{time constant of the second order,}$$

$$T_{1Y} = \frac{b_Y}{k_Y} = \frac{2\delta_Y}{\omega_{0Y}} = 0,0037 \text{ (s)} \quad \dots \dots \dots \text{time constant of the first order.}$$

Corresponding simulation model of the dynamic properties of the servo-cylinder is on the **Fig. 13** in the lower foot. The control unit is modelled by substitutive P- transfer of the first order according to **Fig. 8**.

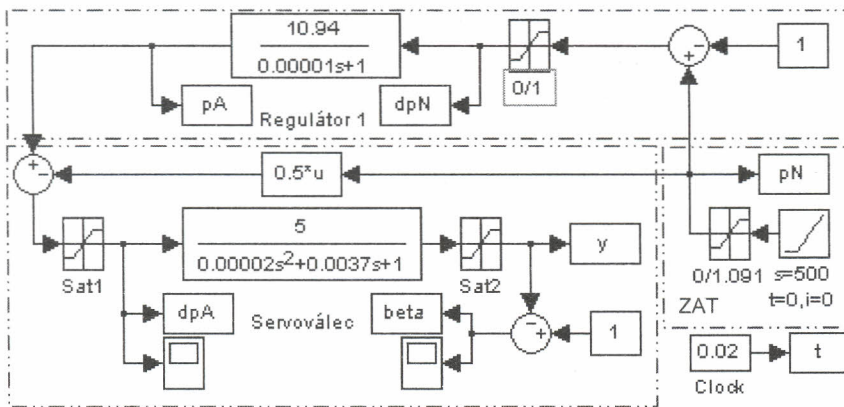


Fig. 13 Simulation model the control unit a servo-cylinder.

In the model of the servo-cylinder, the input limiting block "Sat 1" transmits only positive values of the controlling pressure deviations. The output limiting block "Sat 2" models the mechanical stop of the servo-cylinder stroke.

The results of the simulation is on **Fig. 14** and **Fig. 15**.

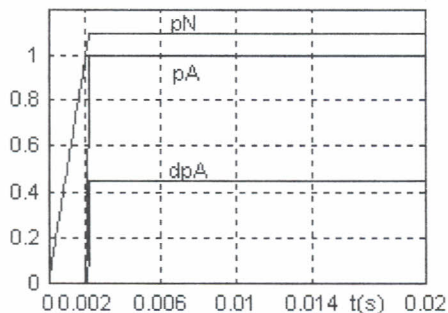


Fig. 14 Input change of the controlling pressure

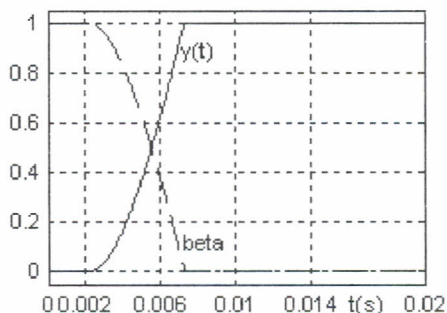


Fig. 15 Time flow of the servo-cylinder stroke

On **Fig. 14** there is generation outlined of the change of the controlling pressure $\Delta p_A = p_A - 0,5 \cdot p_N$ at the servo-cylinder input. The control unit begins generating the controlling pressure p_A as the loading pressure p_N reaches the desired unit value. On **Fig. 15** there is the course of the strike $y(t)$ and dashed course of the dimensionless geometric volume $\beta(t) = 1 - y(t)$.

The model on **Fig. 13** features the source of the loading pressure (ZAT), in the form of ramp function. After the feedback loop is closed, the input ramp of the loading pressure shall be replaced with the source of the loading pressure on the output side of the HGR-O. The loading pressure shall be proportional to the passive moments depending on revolutions and pressure losses at the inner hydraulic HGR-O resistances.

The block to convert the servo-cylinder stroke $y(t)$ to the geometric volume $\beta(t) = 1 - y(t)$ is a part of the closed feedback loop. The passive signum in the given relation determines the signum of the entire feedback. With increasing positive regulation deviation $\Delta p_N(t)$ the geometric volume decreases $\beta(t)$ and thus also the controlled pressure $p_N(t)$ decreases. The feedback is negative.

6. Analysis of the Dynamic Properties of the System

The control unit model and servo-cylinder is supplemented with the HGR-O model with a driving motor and loads. The ZAT 1 load shall model pressure losses at hydraulic resistances depending on the flow and the pressure difference proportional to the passive HGR moments depending on revolutions. Hydraulic resistances against the movement of the liquid are modelled by static function $f(u)=0,8 \cdot u+0,2 \cdot u^2$. The resistance against acceleration of the liquid is modelled with derivative transmission of the first order. The pressure difference depending on revolutions is modelled with multiplier so that it is not necessary to change two parameters at the change of the desired controlled pressure value. The ZAT 2 load shall model effect of connection and disconnection of the hydraulic

motor by moving the distributor. By the latest requirements is adjusted the simulation model at Fig. 16.

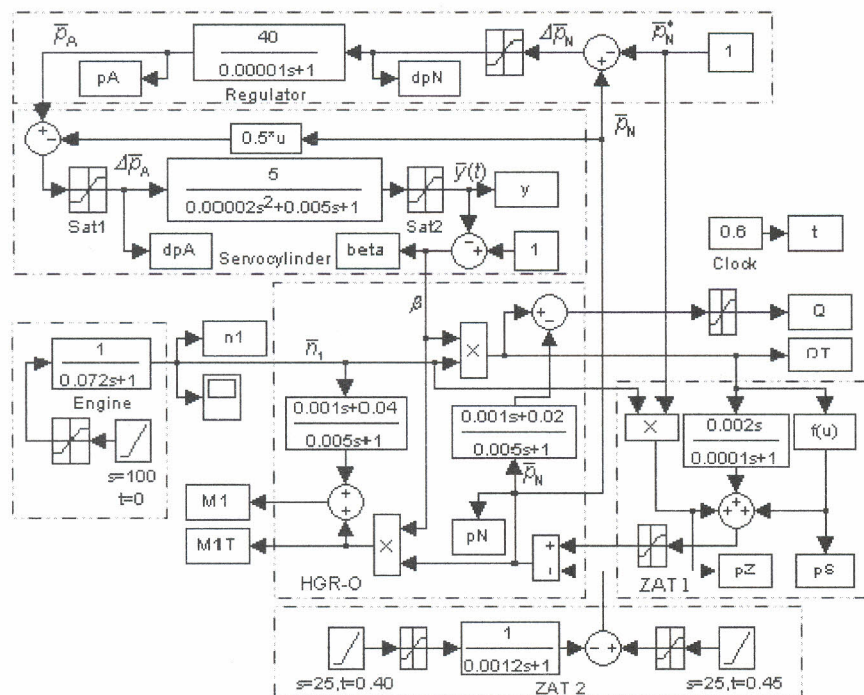


Fig. 16 Simulation model of pressure control system.

The HGR-O Model with driving motor and ZAT 1 load is taken from the study [1] where it is described in details. The driving motor is modelled with a simple image P-transmission of the first order. The inner load ZAT 2 consists of two identical ramps modelling the change of the distributor position. On the left there is the ramp of steepness $s=30 \text{ s}^{-1}$ set for the start time $t_1=0,40 \text{ s}$. The ramp on the left models opening of the distributor and the system pressure drop to the level corresponding to the resistances against the movement of the hydraulic motor. On the right side there is a ramp of the same steepness set for the start time $t_2=0,45 \text{ s}$. The ramp on the right side models transposition of the distributor to the close position or termination of the hydraulic motor stroke by the piston stopped by the lid.

6.1 Closed Distributor Start

First, the system is analyzed at the start of the driving motor and closed RP distributor when the flow of the hydraulic motor is zero ($Q_H=0$) and the whole flow of the hydraulic generator flows through opened negative cover of the controlling edges of the

control unit ($Q_G=Q_N$). The size of this minimal flow is determined by product of velocities of servo-cylinder movement and its active area S_{Y1} . In the dimensionless form it is $\bar{Q}_N(t)=\bar{y}(t)$. In the ZAT 1 Load it is modelled by function $f(u)$ where $u=\bar{Q}_N(t)$. The effect of the change of distributor position is eliminated through setting of start time in the ZAT-2 ramps longer than the start simulation time. The motor is started in time $t_0=0$ s. The results of simulation are on the following figures:

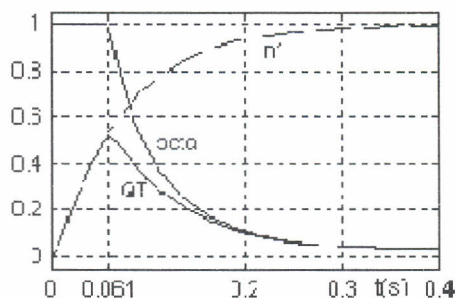


Fig. 17 Revolutions, geometric volume and flow

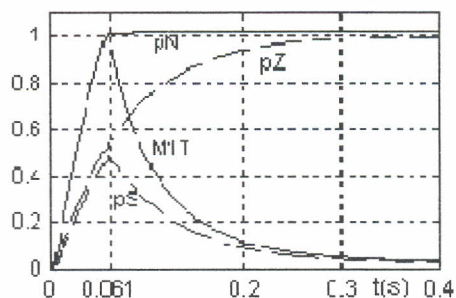


Fig. 18 Controlled pressure and moment

The pressure control unit begins affecting in the time $t_1=0.061$ s when the system pressure reaches the desired value. Until then the servo-cylinder stroke is zero while the geometric volume is maximal and all the quantities are increasing.

As soon as the pressure control unit starts its performance, the geometric volume and flow on Fig. 14 begins decreasing. On Fig. 15 there is the controlled pressure p_N maintained on the constant value while the moment is decreasing. For dimensionless flow on the Fig. 14 stands the definition relation $\bar{Q}_T = \bar{n}_1 \cdot \beta$. In the range $t \in \langle 0, t_1 \rangle$ there is $\beta=1$ and $\bar{Q}_T = \bar{n}_1$. In the range $t \in \langle t_1, \infty \rangle$ the flow course is according to the definition relation. Similarly, it stands for the moment $\bar{M}_{1T} = \bar{p}_N \cdot \beta$. At $\beta=1$ is $\bar{M}_{1T} = \bar{p}_N$. At $\bar{p}_N=1$ is $\bar{M}_{1T} = \beta$.

The geometric volume and flow do not decrease to zero. To maintain the constant pressure the control unit requires the minimal flow through negative cover of opened controlling edges. Then on Fig. 17 neither the theoretic moment shall drop to the zero value. The greater the statistic deviation is, the greater the non-zero value of controlled quantities in the new balanced state is. Therefore, in tuning the model on Fig. 16 the proportional amplification of the control unit was increased.

6.2 Deferred Start and Lowered Desired Value

The system simulation model on Fig. 15 is functional even at lowered desired value of the controlled pressure and in time deferral of the driving motor start. On the

following Figure there are results of the simulation if $p_N^*=0.8$ and on the start of the motor deferred to the time $t_2=0,05$ s.

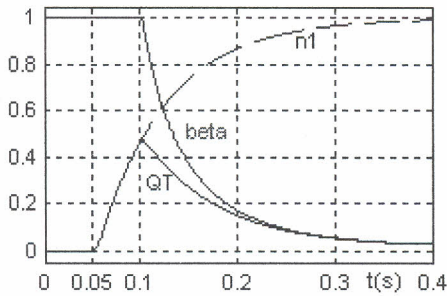


Fig. 19 Revolutions, the geometric volume and flow

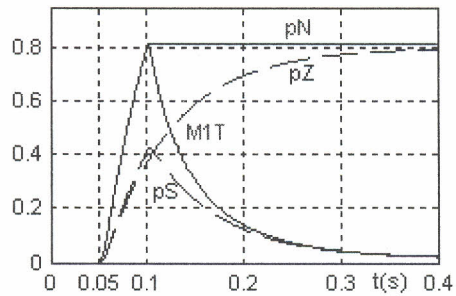


Fig. 20 Pressures and the controlled moment

The start of all the characteristics is deferred by $\Delta t = 0.05$ s. Lower desired value of the controlled pressure p_N^* corresponds to the lower values of all the other pressures as well as the lower value of the moment maximum. Slightly shorter is the time of the start. It is important that prior to the start, according to the simulation results on GHR-O, the maximal geometric volume and all the other quantities are zero as it is in accordance with to the reality.

6.3 Putting the Hydraulic Motor into Operation

The driving motor gets started in the time $t_0=0.05$ s. The desired value of the controlled pressure shall be per unit. With constant revolutions, the RP distributor moves to the open position in the time $t_2=0.4$ s. In the time $t_3=0.45$ s the distributor moves to the closed position or the hydraulic motor stroke is stopped when the piston hits the lid. The time $t_3=0.45$ s is the starting time of the ramp on the right side in the ZAT 2 load in the model on **Fig. 16**. The hydraulic motor stops, the system pressure stops, the system pressure increases while the pressure control unit restores its activity.

The inner load ZAT 2 consists of two identical ramps modelling the change of the distributor position. On the left side there is a ramp set for the starting time $t_2=0.40$ s. The ramp on the left side models opening of the distributor and decrease of the system pressure to the level corresponding to the resistances against the movement of the hydraulic motor.

Resistances against the movement of the hydraulic motor are modelled with the P-transmission of the first order. Increase in pressure below the desired value disables the pressure control unit. The controlling pressure p_A drops to the zero value and the swing board turns over to the maximum position. There is no flow flowing through the closed regulator. Starting from the time $t_1=0.4$ s the whole flow of the hydraulic generator is

transferred to the hydraulic motor input. ($Q_G=Q_H$). Until the time $t_1=0.4$ s the courses of characteristics are identical to those on **Fig. 16** to **Fig. 19**.

On the right side there is a ramp of the same steepness set for the start time $t_3=0,45$ s. The ramp on the right side models the shift of the distributor to the closed position or termination of the hydraulic motor stroke when the piston hits the lid. With the distributor closed, the system pressure increases and after the desired value of the controlled pressure is exceeded, the control unit restores its activities. It overturns the swing board to the zero position while maintaining the controlled pressure on the constant value. With the constant value of the controlled unit maintained, the minimal flow controls through open controlling edges the slide valve which is the part of the flow flowing through loading resistances. For activation of the ZAT 2 load, the simulation time just increases for the simulation model on **Fig. 16**.

The result of the simulation:

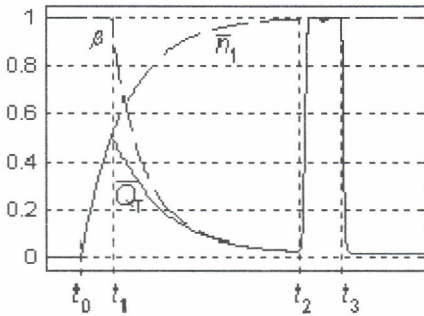


Fig. 21 Revolutions, the geometric volume a flow.

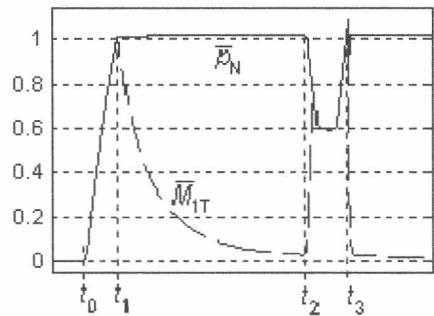


Fig. 22 The controlled pressure and momen

Marked times:

t_0 - start of the motor

t_1 - start of the control unit

t_2 - hydraulic motor start and control unit stop. (Opening the distributor).

t_3 - hydraulic motor stop and control unit start. (Closing the distributor).

On **Fig. 21** there is a course of quantities from the definition relation $\bar{Q}_T = \bar{n}_1 \cdot \beta$. In the time $t_2=0.4$ s the revolutions are already per unit and the course of the flow is identical to the course of the geometric volume. With the distributor opening in the time $t_1=0.4$ s with constant revolutions the geometric volume and flow increase up to the maximal value. With the distributor closed in the time $t_2=0.45$ s, the flow through the hydraulic motor Q_H resets. The pressure increases and the control unit turns over the board to the

minimum position corresponding to the minimal flow Q_N through the negative cover of the controlling edges of the control unit.

On **Fig. 22** there is a corresponding course of the controlled pressure p_N and the theoretical moment. There applies a definition relation $\overline{M}_{1T} = \overline{p}_N \cdot \beta$. If $\beta = 1$ then $\overline{M}_{1T} = \overline{p}_N$. If $\overline{p}_N = 1$ then $\overline{M}_{1T} = \beta$.

On **Fig. 23** there are sections shown of the dynamic characteristics as outlined in the technical documents of the HGR-O producers [5].

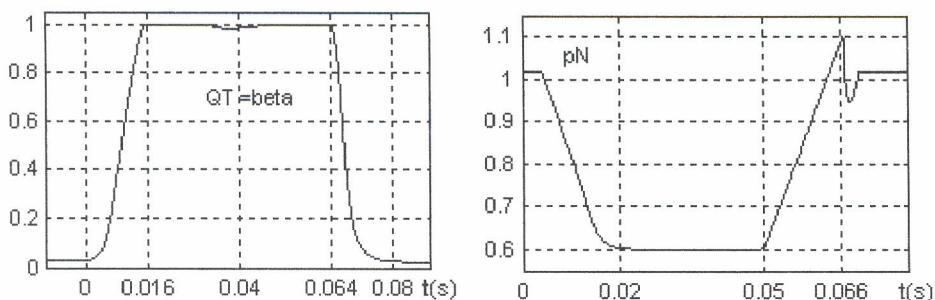


Fig. 23 Detail of dynamic characteristics of flow and control pressure

According to the final Figure, the pressure control unit with preset parameters turns over the board in the both directions in about 16 ms. The results of the simulation on the final figure correspond rather well with the results of the measuring as stated in the catalogue documents by the HGR producers. If the hydraulic motor is idle, the driving motor is loaded with a nonzero moment just for a very short time of the transient act. (On the start and close of the distributor). In steady states, the hydraulic generator regulating the constant pressure loads the driving motor with theoretically zero moment. No "LS" distributor is capable of that in the open circuit with non-regulating gear hydraulic generator. There is no distributor in the closed hydraulic circuits of the HS gearings. Regulation to the constant pressure is a basis of the energy-saving hydraulic systems.

Submitted: 22.2.2009

References

1. KOREISOVÁ, G. *Nonlinear model of regulation hydrogenerator*. Slovak Society for H+P, Acta hydraulica et pneumatica. 1/2008. ISSN 1336-7536.
2. KOREISOVÁ, G. *Identification of viscous damping coefficient of hydraulic motors*. Sci Pap 12 (2006), p. 61, ISSN 1211-6610.

3. KOREIS, J., KOREISOVÁ, G. *Hydrostatické mechanizmy v konstrukci vozidel*. HYDROPNEUTECH s.r.o. Žilina, (2004), s.85-118, ISBN 80-968961-1-3.
4. TURZA, J. *Dynamický model rotačného hydrostatického prevodu s obmedzením maximálneho tlaku riadením*. Habilitačná práca. VŠDS Žilina, (1992).
5. On-line: <http://www.boschrexroth.com/>, <http://www.hytos.cz/>.

Resumé

SYSTÉM AUTOMATICKÉHO ŘÍZENÍ TLAKU

Gabriela KOREISOVÁ, Josef KOREIS

Článek popisuje statické a dynamické vlastnosti systému řízení tlaku v otevřeném hydraulickém obvodu s regulačním hydrogenerátorem. Nejprve jsou sestaveny simulační modely statických a dynamických vlastností regulátoru tlaku a ovládacího servoválce hydrogenerátoru. Následně je sestaven simulační model statických a dynamických vlastností celého systému automatického řízení tlaku.

Summary

AUTOMATIC PRESSURE CONTROL SYSTEM

Gabriela KOREISOVÁ, Josef KOREIS

The article describes static dynamic properties of the pressure control system in an opened hydraulic circuit with a regulating hydraulic generator. First, simulation models are assembled of static and dynamic properties of the pressure control unit and controlling servo-cylinder of the hydraulic generator. Subsequently, a simulation model is assembled of the static and dynamic properties of the entire automatic pressure control system.

Zusammenfassung

AUTOMATISCHES DRUCKSTEUERUNG SYSTEM

Gabriela KOREISOVÁ, Josef KOREIS

Das Artikel beschreibt statische und dynamische Eigenschaften Des Drucksteuerung System in offenem hydraulischen Kreislauf mit regelbarer hydrostatischen Pumpe. Zuerst die Simulationsmodellen für statische und dynamische Eigenschaften für Druckregler und Servozylinder der Pumpen zusammengestellt. Dann ist ein Simulationsmodell für statische und dynamische Eigenschaften des ganzen Automatischen Drucksteuerung Systems zusammengebaut.